Femtochemistry

Atomic-Scale Dynamics of the Chemical Bond

Ahmed H. Zewail

J. Phys. Chem. A, 104(24), 5660-5694, 2000

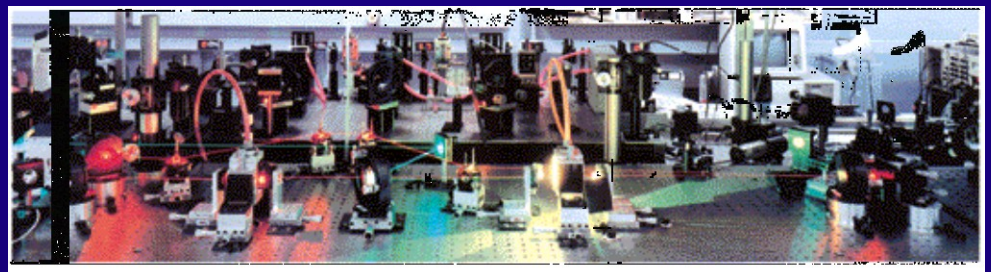

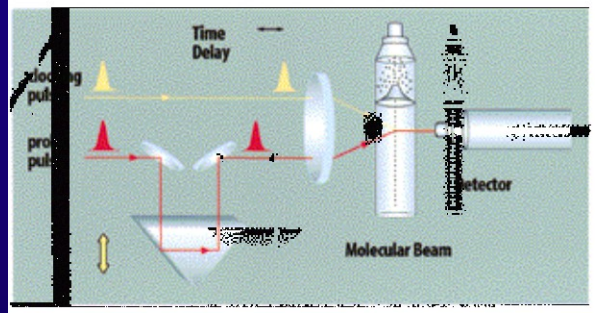

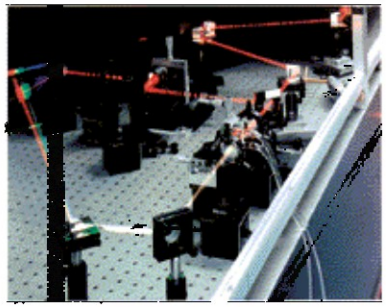

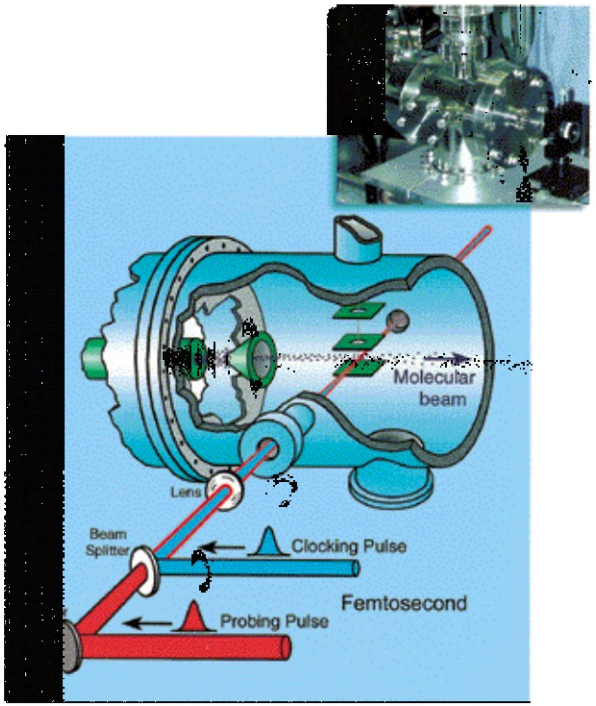

Figure 1
Femtochemistry apparatus, typical of early Femtolands. Laser system: (top) the first CPM oscillator used in Femtoland I; *(bottom)* the continuum generation to the right and the experimental layout for clocking, to the left. Molecular beam apparatus of Femtoland III, together with a view of the beam/laser arrangement.

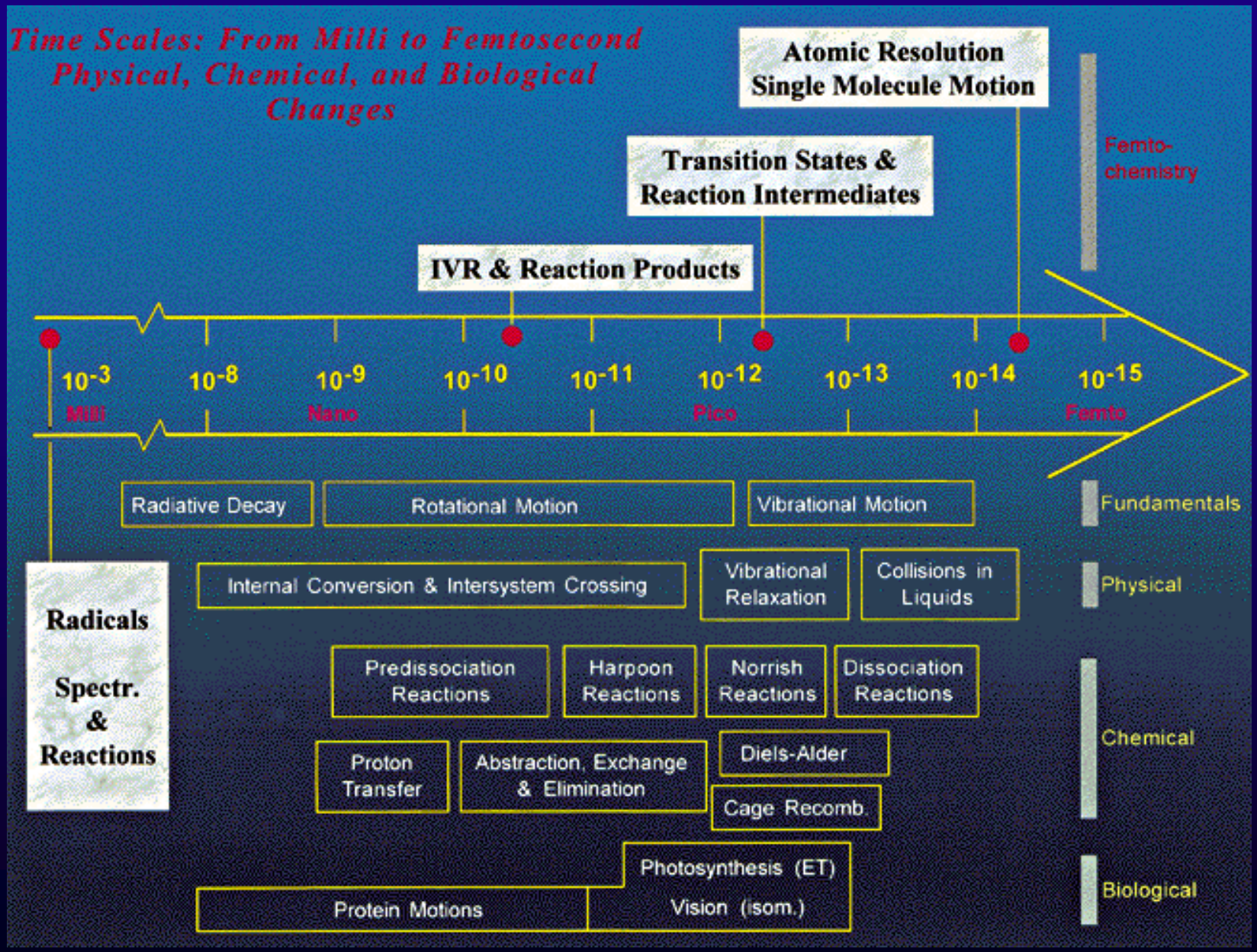

Figure 2 Time scales. The relevance to physical, chemical, and biological changes. The fundamental limit of the vibrational motion defines the regime for femtochemistry. Examples are given for each change and scale.

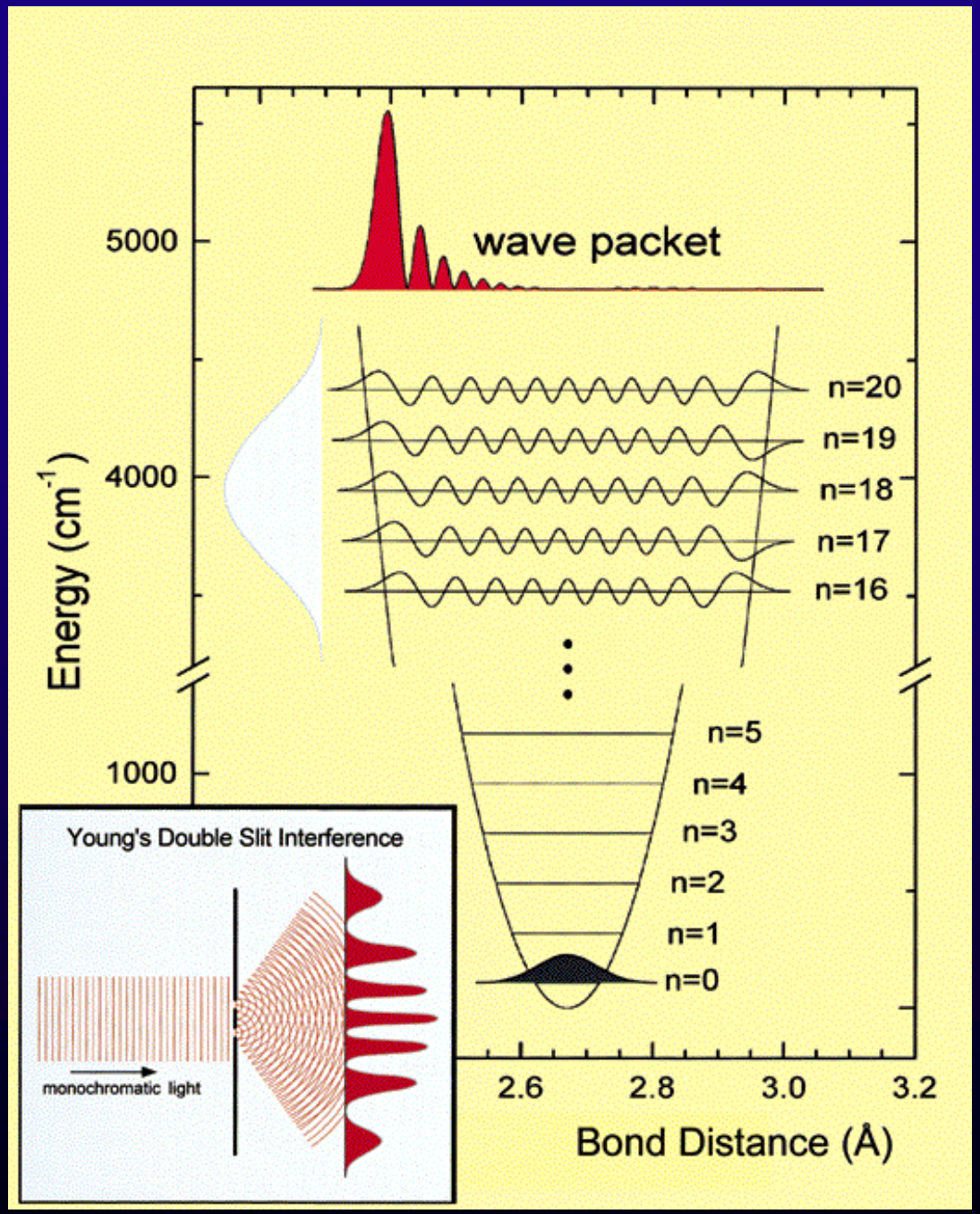

Figure 3
Coherent, localized wave packet (de Broglie length ~0.04 Ĺ) calculated for a diatomic molecule (iodine) for a 20 fs pulse. The kontrast with the diffuse wave function limit (quantum number n) is clear. The inset shows Thomas Young's experiment (1801) with the interference which is useful for analogy with light. Reference 39

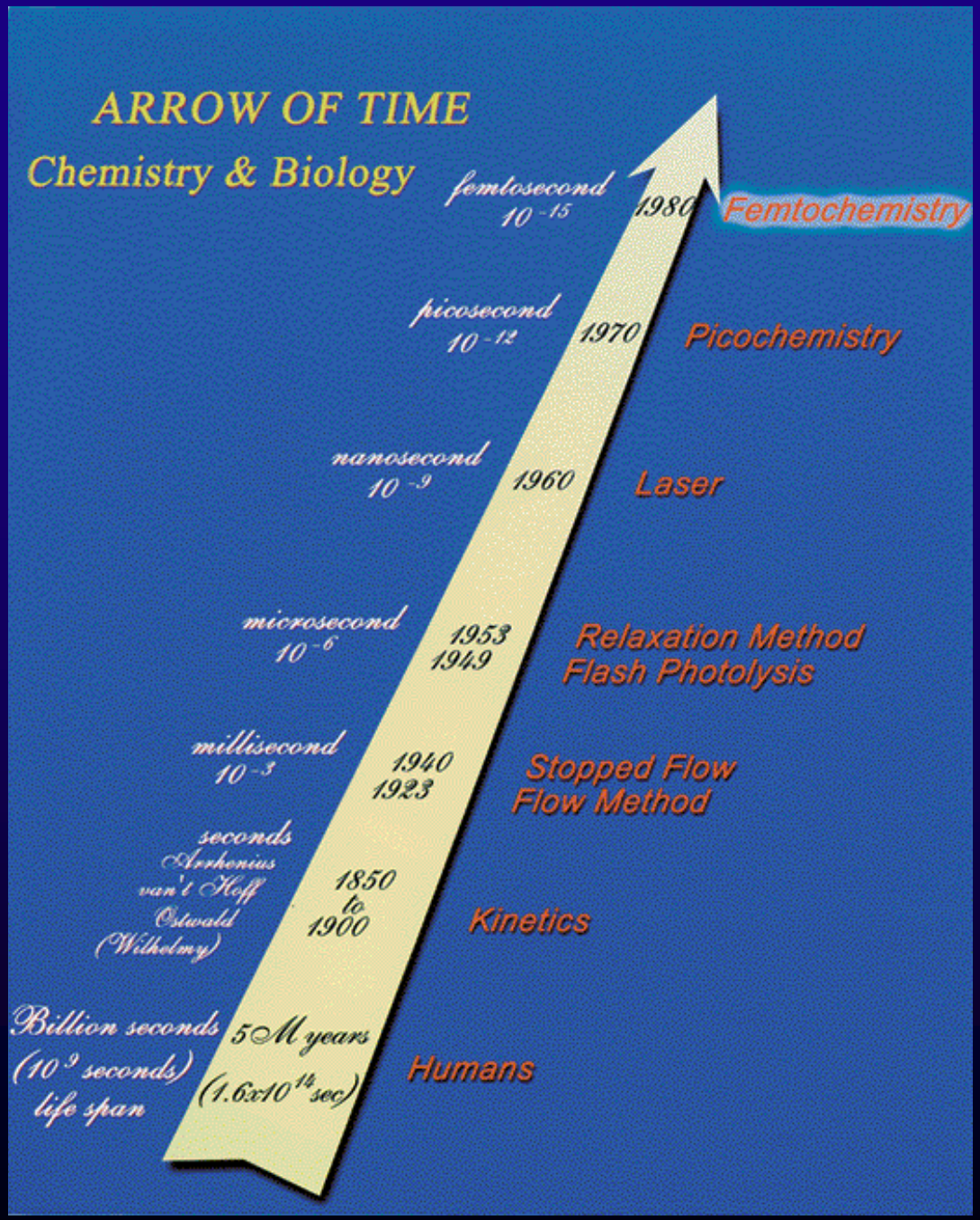

Figure 4
Arrow of time in chemistry and biology, some steps over a century of development.

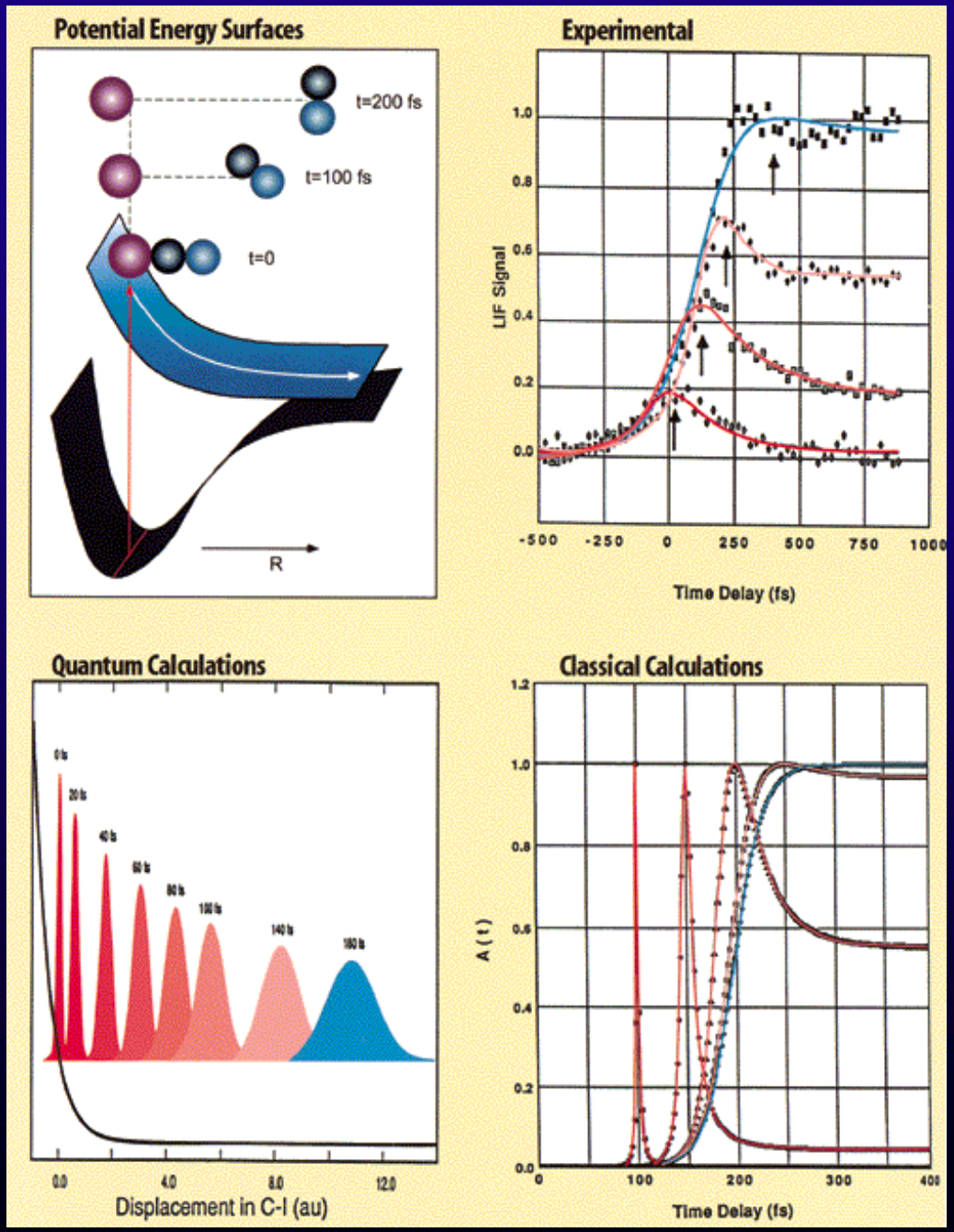

Figure 6

Femtochemistry of the ICN reaction, the first to be studied. The experimental results show the probing of the reaction in the transition-state region (rise and decay) and the final CN fragment (rise and leveling) with precise clocking of the process; the total time is 200 fs. The I fragment was also detected to elucidate the translational energy change with time. Classical and quantum calculations are shown. Reference 41.

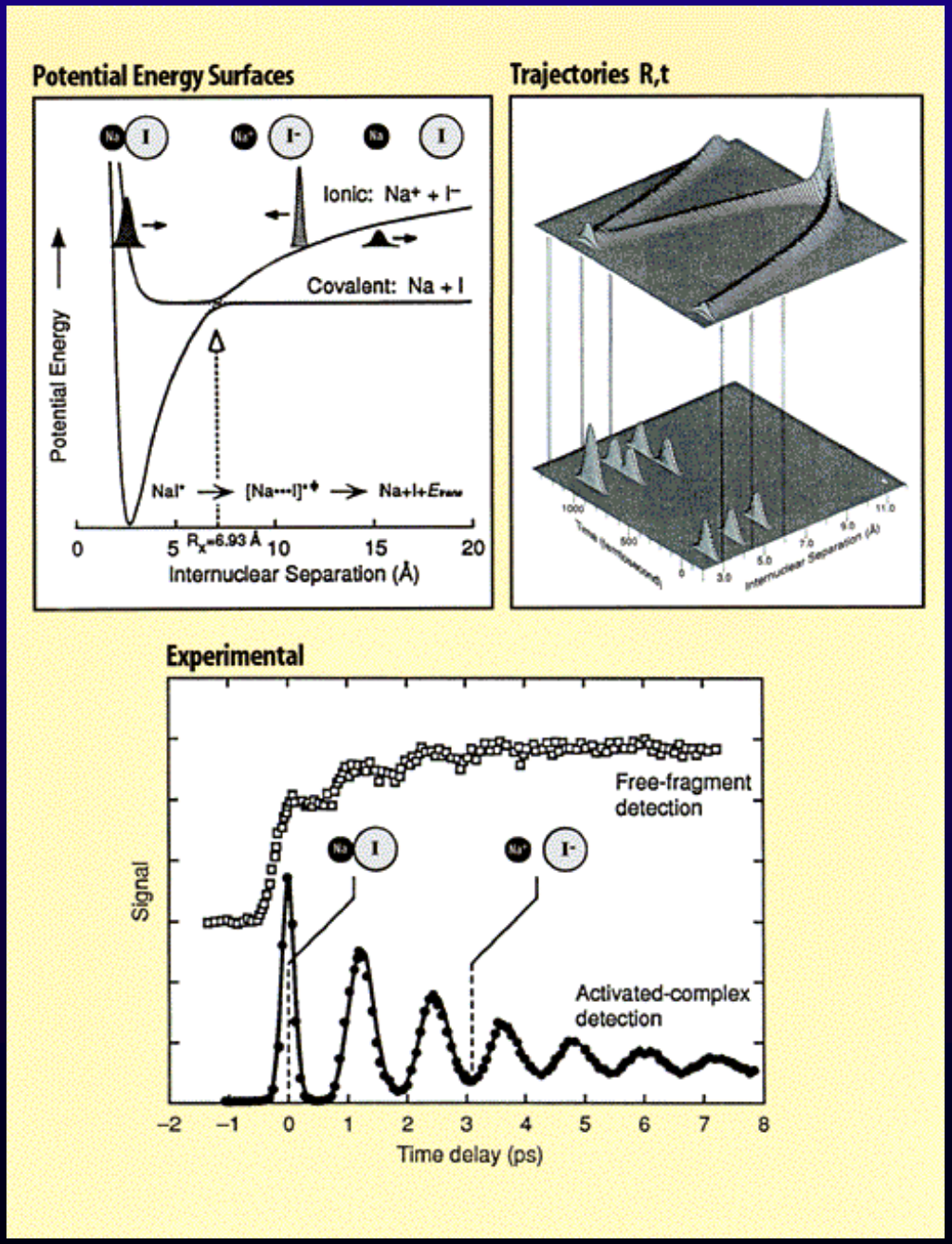

Figure 7

Femtochemistry of the NaI reaction, the paradigm case. The experimental results show the resonance motion between the covalent and ionic structures of the bond, and the time scales for the reaction and for the spreading of the wave packet. Two transients are shown for the activated complexes in transition states and for final fragments. Note the "quantized" behavior of the signal, not simply an exponential rise or decay of the ensemble. The classical motion is simulated as trajectories in space and time. Reference 42.

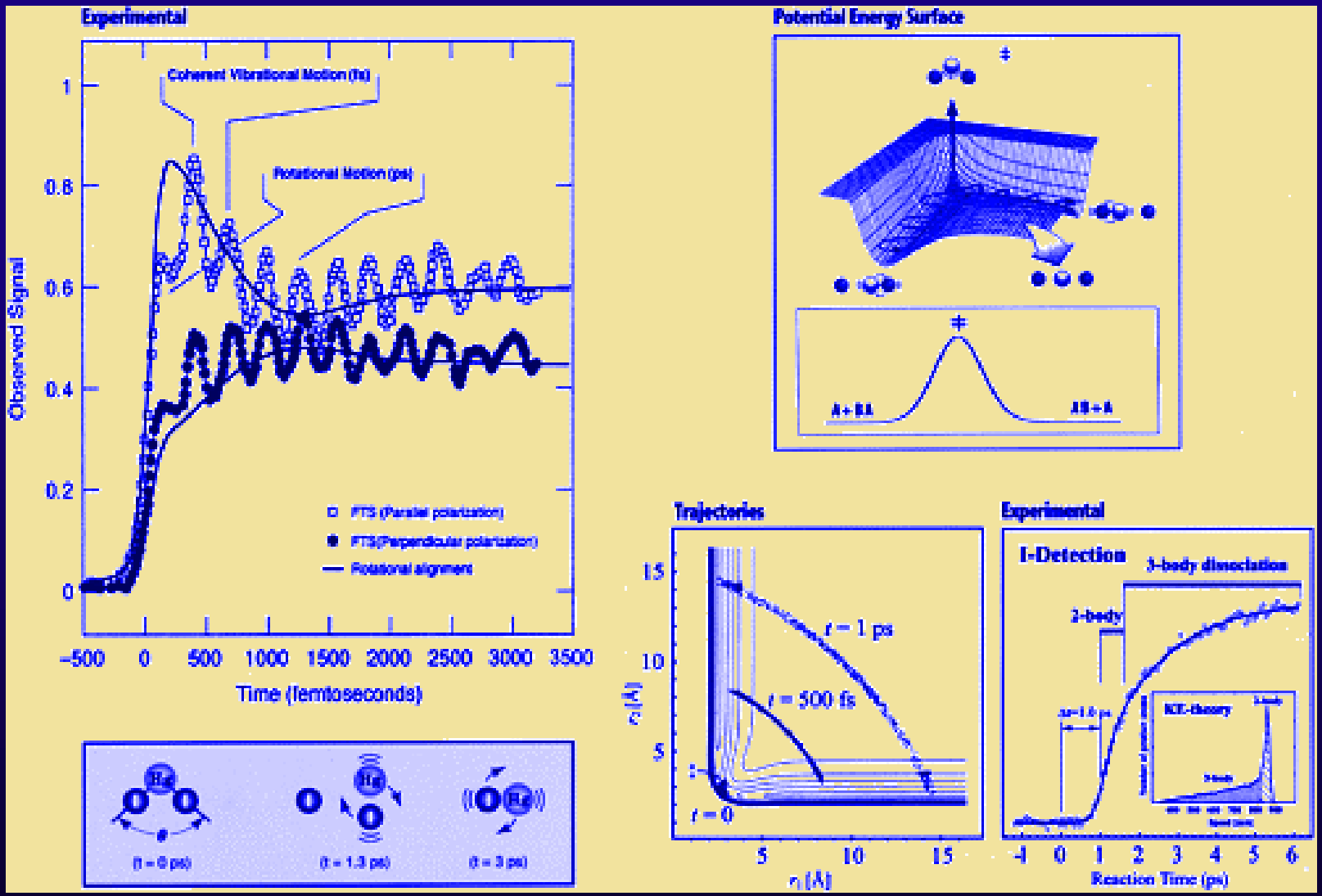

Figure 8 Femtochemistry of the IHgI reaction, the saddle-point transition state (barrier reactions). The experimental results show both the coherent vibrational and rotational motions of the reaction (left). The transition state IHgI* and final fragment HgI were probed. We also probed the I fragment and the change of translational energy with time. The classical trajectory calculations are shown (right), together with experimental results for I detection; both theory and experiment illustrate the family of reaction trajectories on the global PES, in time and in kinetic energy distribution. Quantum calculations were also made (not shown). This ABA system is a prototype for saddle-point transition states. Reference 43.

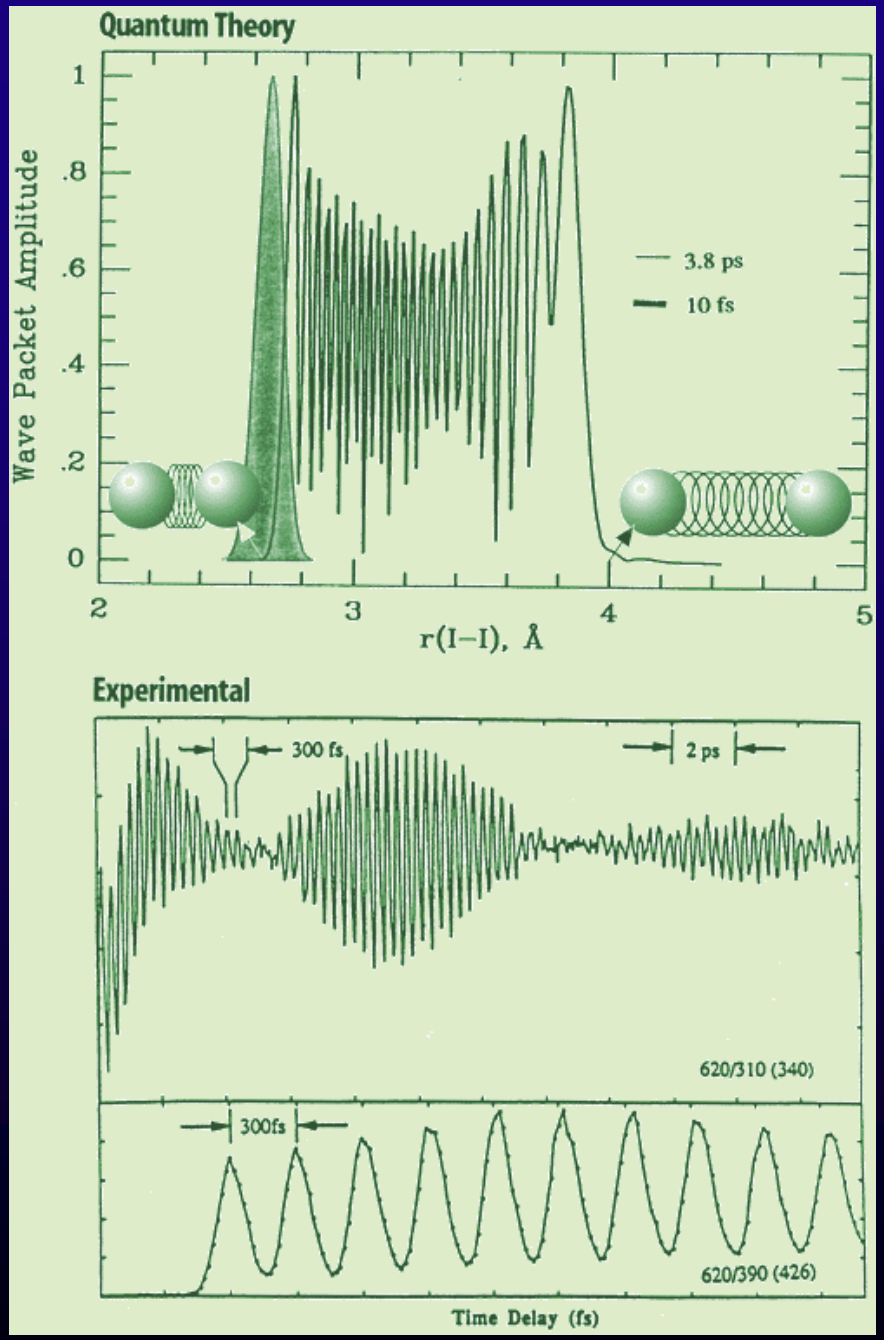

Figure 9

Femtosecond, real time observation of the vibrational (and rotational) motion of iodine. The experiments show the anharmonic nature of the bound motion. Quantum theory indicates the limit for creating a localized wave packet on the femtosecond time scale. The localized wave packet describes the classical spring motion. Reference 44.

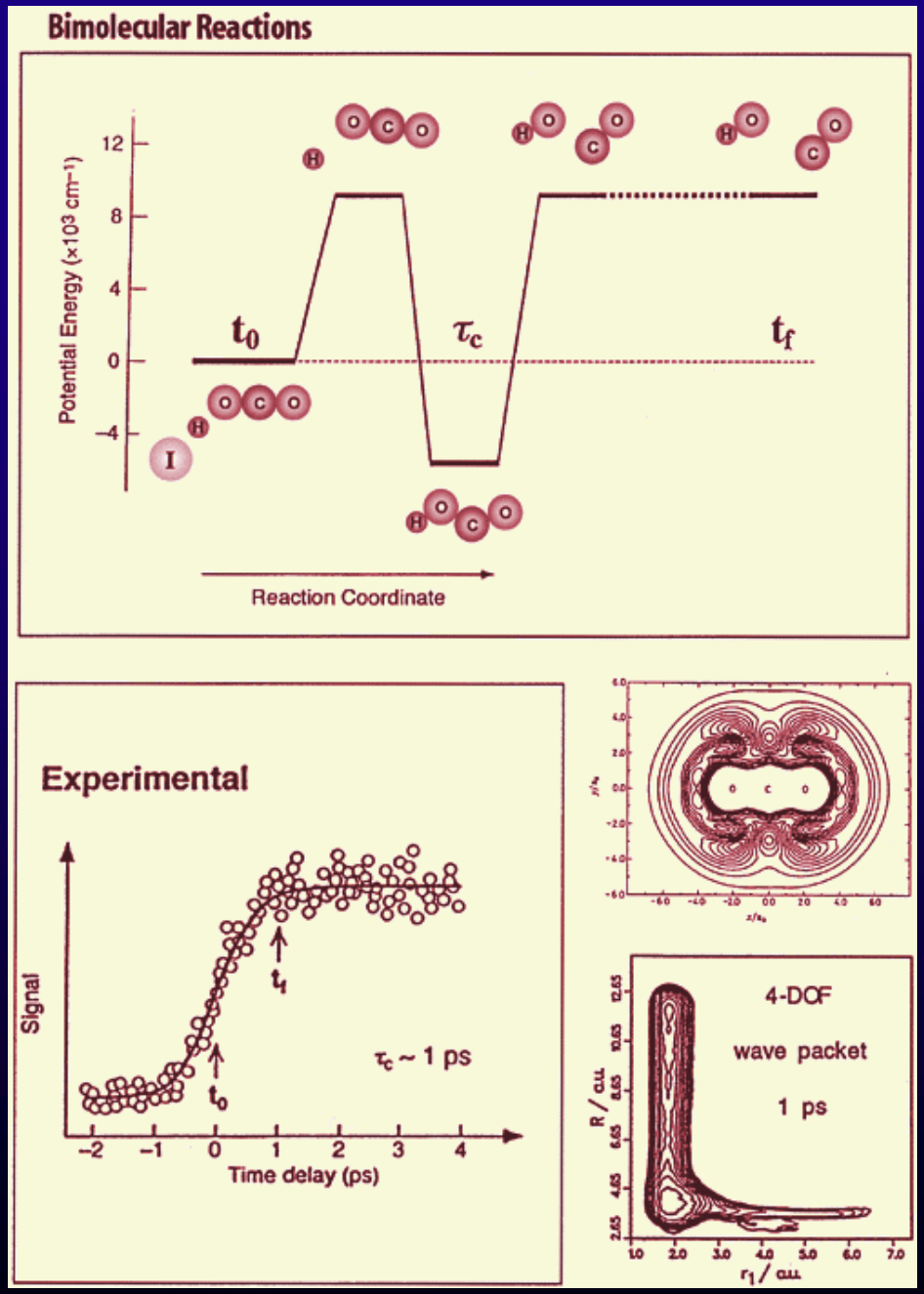

Figure 10

Femtochemistry of the bimolecular $H + CO_2$ reaction. The precursor in this molecular beam experiment is HI/CO_2 in a van der Waals complex. The initial experiments utilized picosecond pulses, but later subpicosecond pulses were used (see text). Theoretical ab initio calculations of the PES and the dynamics (classical, semiclassical and quantum wave packet) have all been reported (see text). The transit species HOCO lives for ~1 ps. Similar studies were made of reactive $Br + I_2$, of the inelastic collision between I and CH_3I, and of other bimolecular reactions. Reference 45.

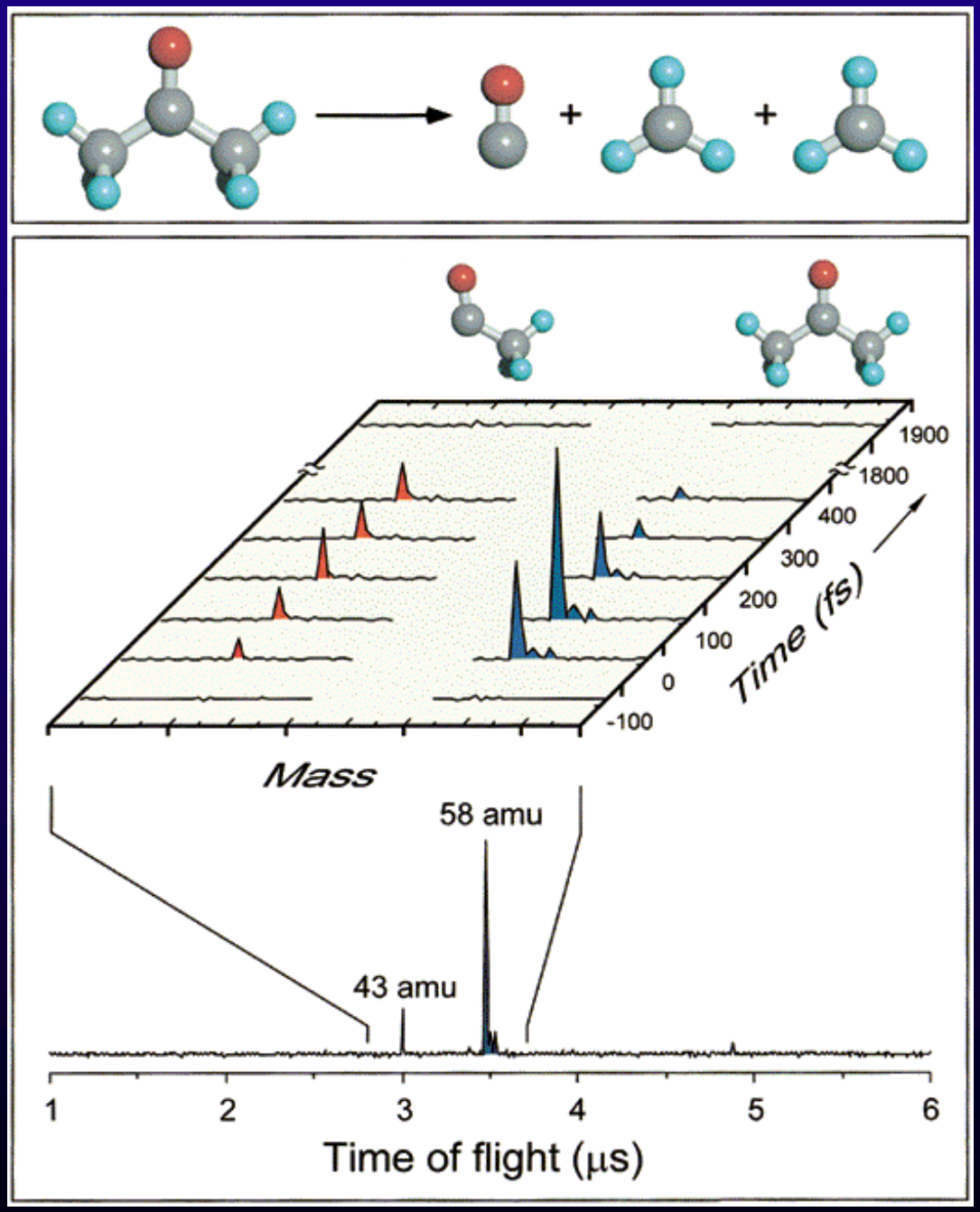

Figure 11

Femtosecond mass spectrometry, a 2D correlation important in the studies of reactive intermediates. The example given here is for the reaction of acetone (Norrish-type I) and its nonconcerted behavior. Reference 46.

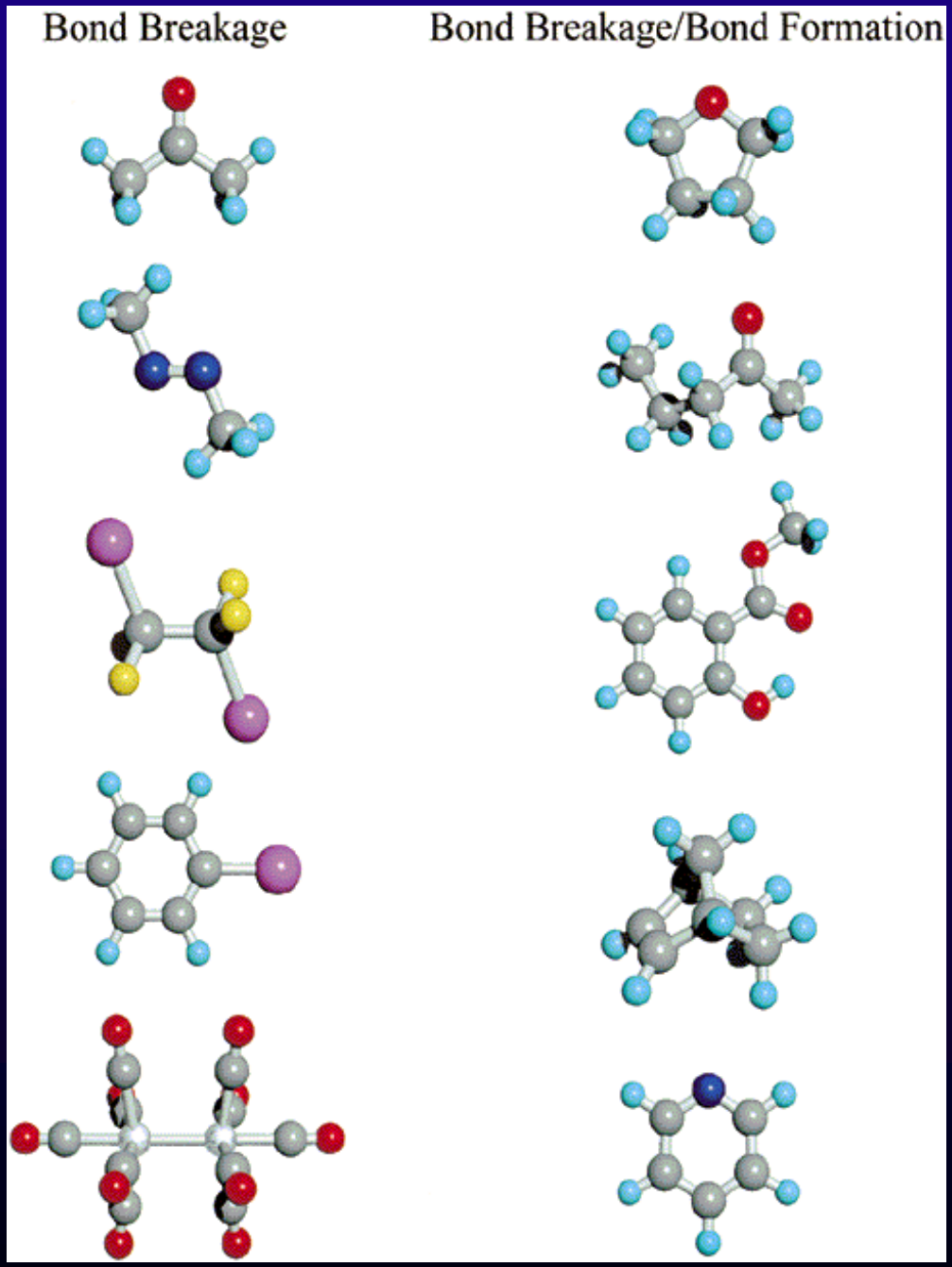

Figure 12

Molecular structures of different reactions studied, typical of the systems discussed in the text for organic and organometallic femtochemistry: acetone; azomethane; diiodoethane; iodobenzene; $Mn_2(CO)_{10}$; cyclic ethers; aliphatic ketones for Norrish-II reactions; methyl salicylate; one of the structures studied for addition and elimination reactions; pyridine for valence isomerization.

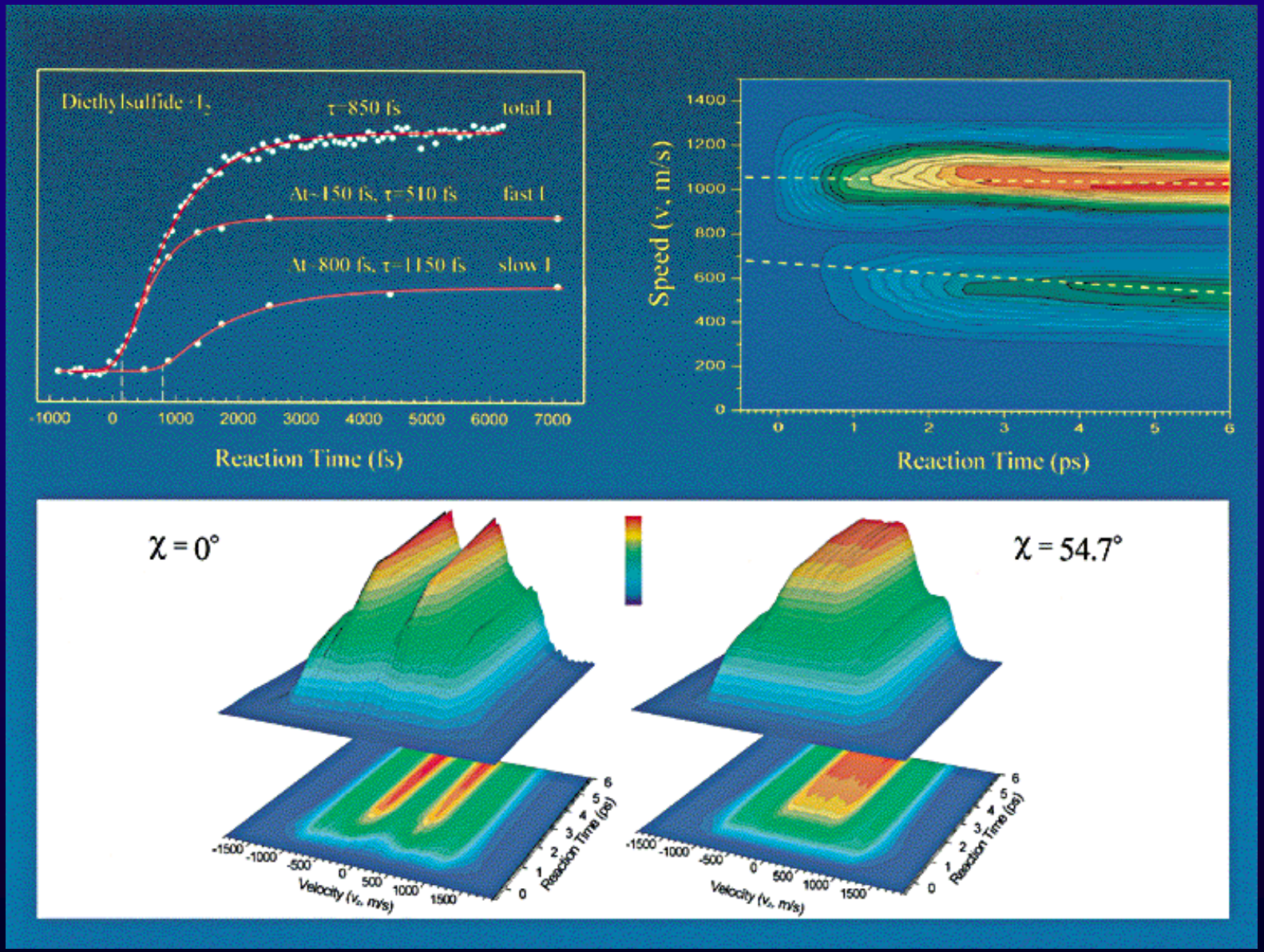

Figure 13 Femtochemistry of bimolecular electron-transfer reactions, the classic case of donors (e.g., benzene or diethyl sulfide) and acceptors (e.g., iodine or iodomonochloride). The experimental results clearly show the distinct velocity and time correlations, and thus the two-speed distributions and time scales of the reaction on the global PES. Reference 47.

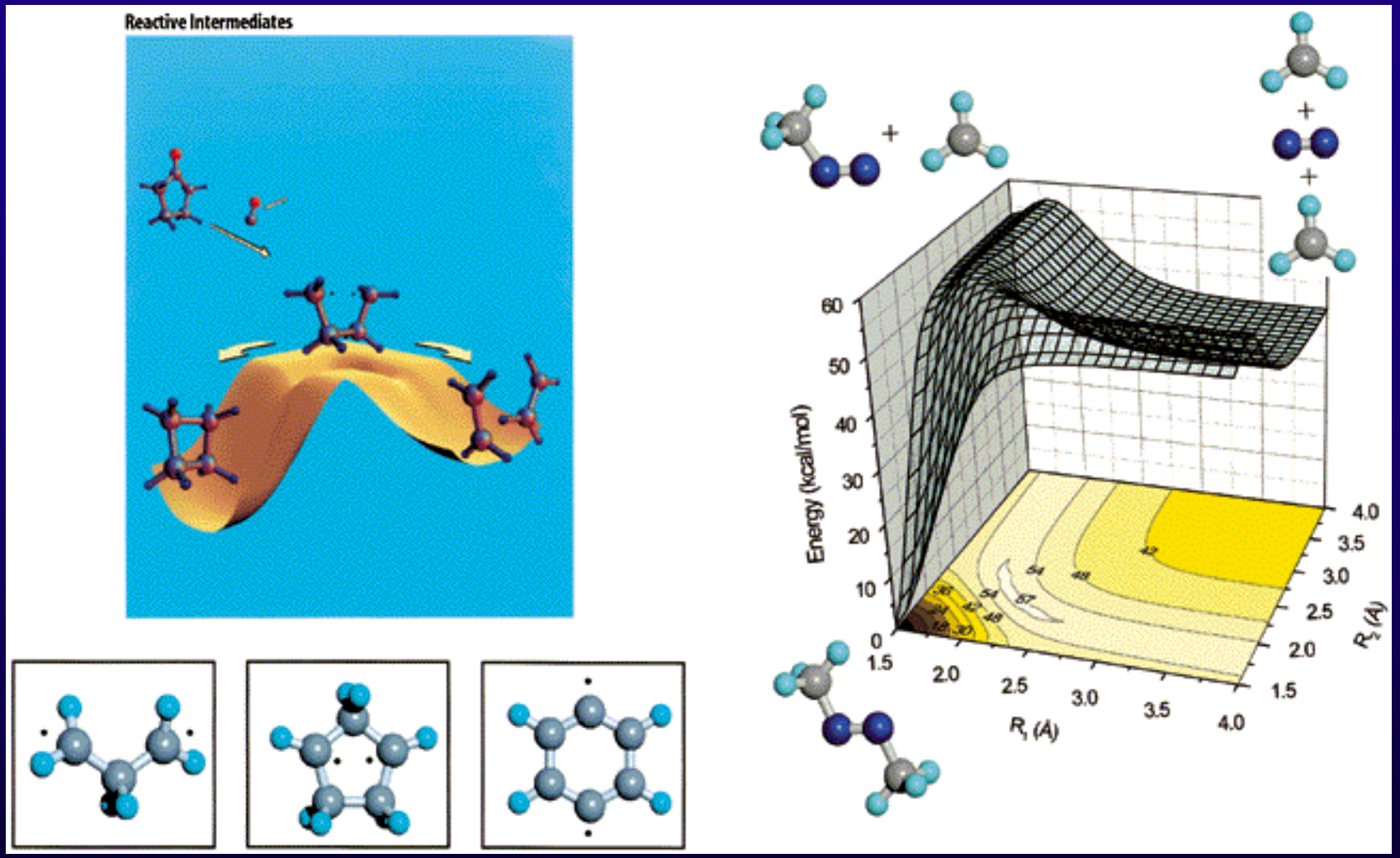

Figure 14 Reactive intermediates on the femtosecond time scale. (Left) Here, tetramethylene, trimethylene, bridged tetramethylene and benzyne are examples of species isolated on this time scale (see Figure 12 for others). (Right) Reaction dynamics of azomethane, based on the experimental, femtosecond studies. The ab initio PES was obtained from state-of-the-art calculations (E. Diau, this laboratory) which show the two reaction coordinates (C-N) relevant to the dynamics. A third coordinate, which involves a twisting motion, was also studied. Note the concerted and nonconcerted pathways. Reference 48.

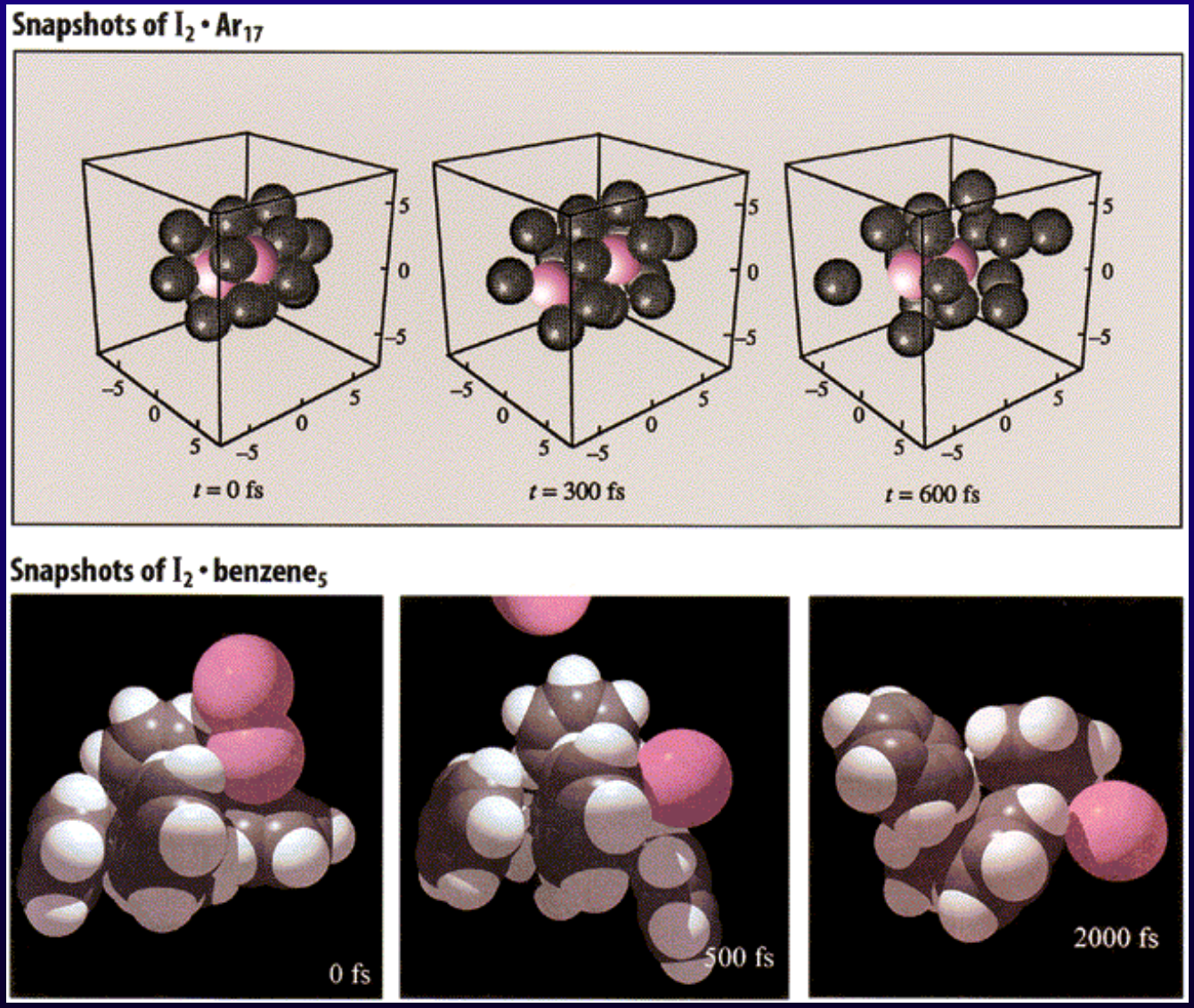

Figure 15 Femtosecond dynamics in the mesoscopic phase, reactions in solvent clusters. Two examples are given: The coherent nuclear dynamics of bond breakage and recombination of iodine in argon (the cage effect), and the dynamics of the same solute but in polyatomic solvents (benzene). It was for the former that the first coherent bond breakage in the cage was observed and separated from the effect of vibrational relaxation. For the latter, the two atoms experience different force fields and the time scales are determined by the degree of solvation. (We also studied van der Waals complexes.) Studies of acid-base reactions of naphthol with ammonia, changing the number of solvent molecules from 0 to 10, and the isomerization of stilbene (hexane as a solvent) were similarly made. Reference 49.

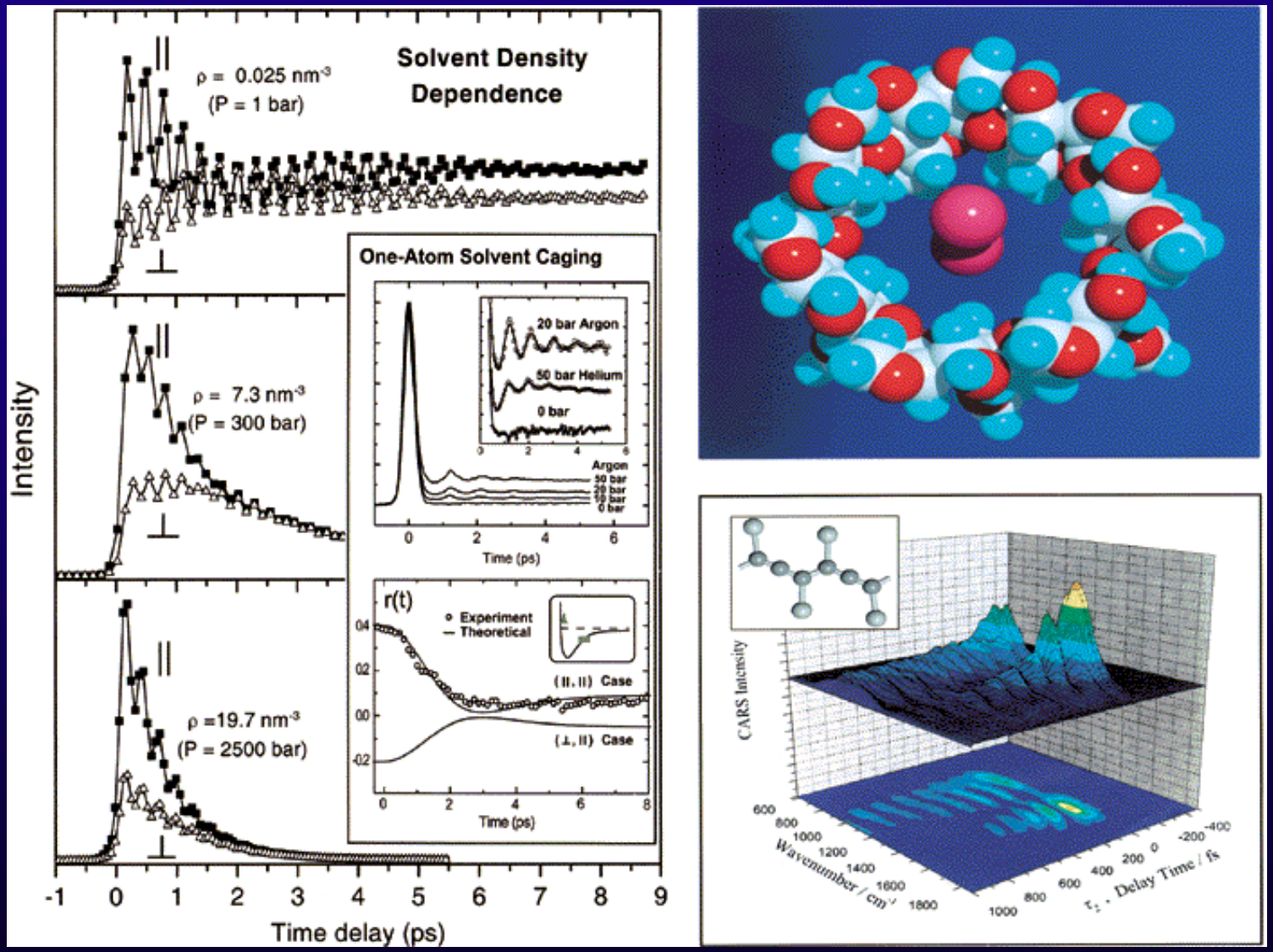

Figure 16 Femtosecond dynamics in the condensed phase: (left) coherent vibrational and rotational motions observed in dense fluids as a function of density and down to the one-atom collision with iodine; (right) nanocavities of cyclodextrins and polymers of polydiacetylenes; liquids (not shown, but references are given). Studies in these media include the one-atom coherent caging, J-coherence friction model, coherent IVR in polymer chains, and anomalous T2 behavior in dense fluids. Reference 50.

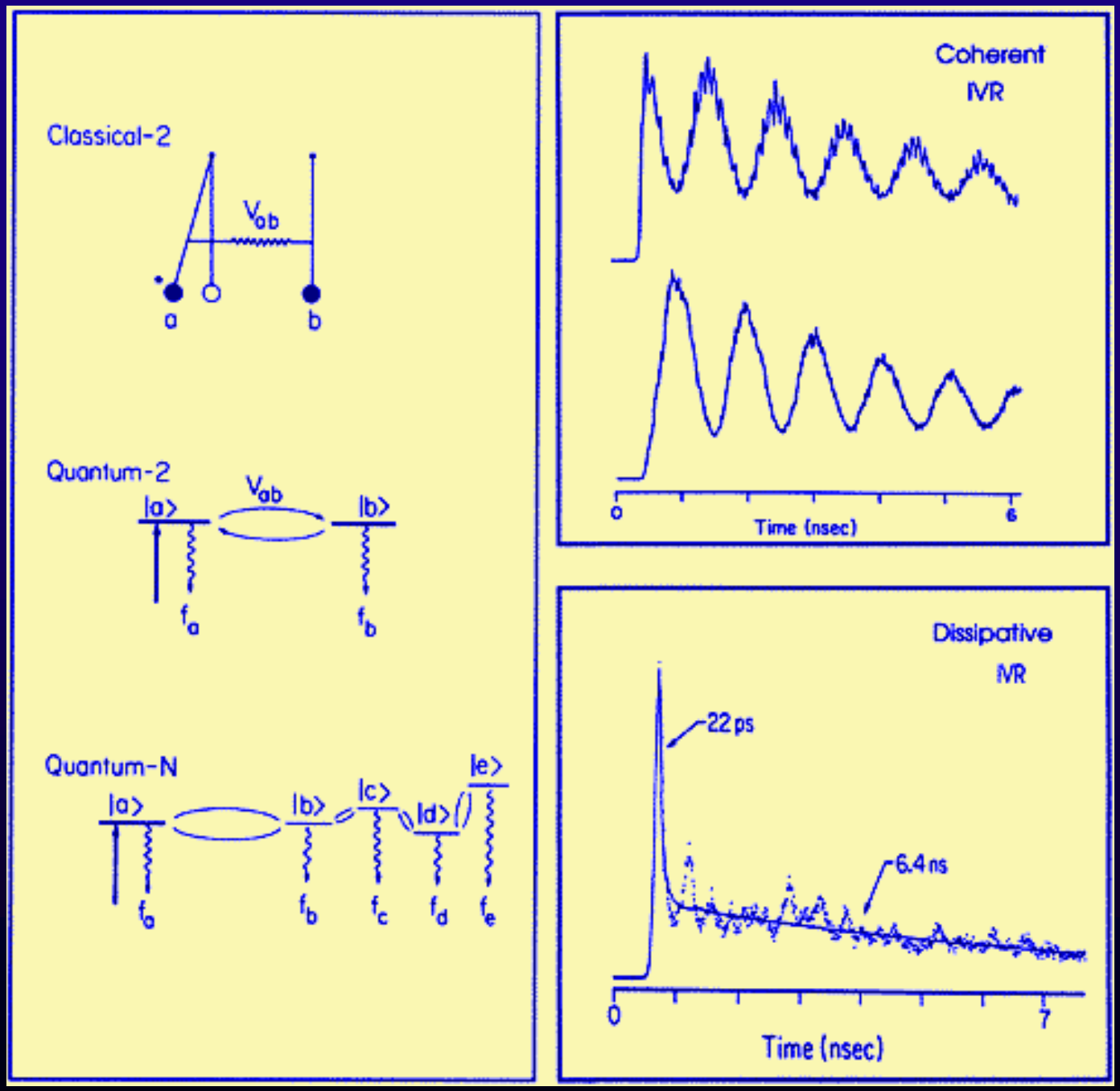

Figure 5

Dynamics of IVR, intramolecular vibrational-energy redistribution. The coherent, restricted, and dissipative regimes. Note the exact in-phase and out-of-phase oscillatory behavior between the vibrational states of the system (anthracene in a molecular beam). The theory for classical and quantum pictures (to the left) has been discussed in detail in the references given. Reference 40.

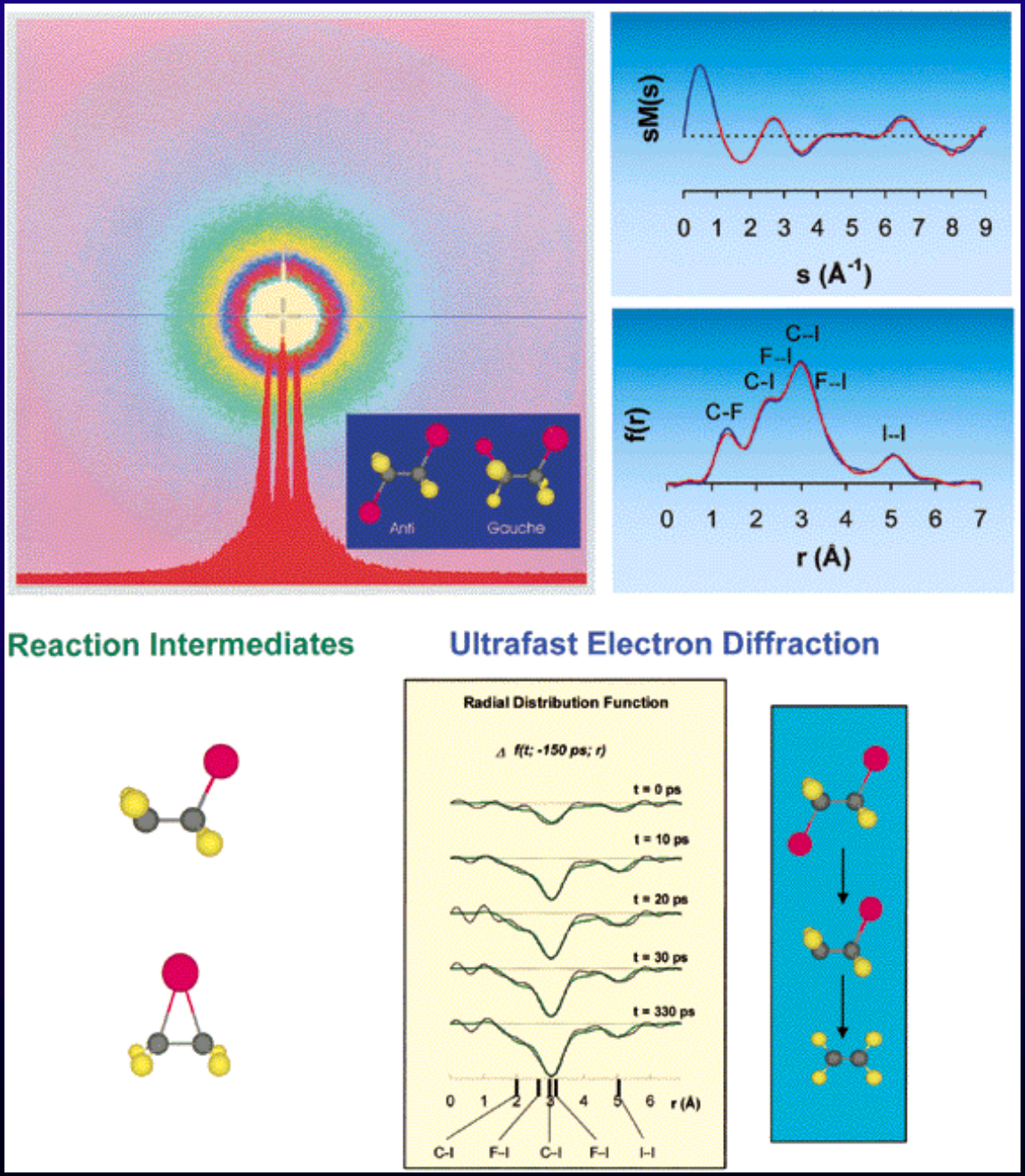

Figure 17

Ultrafast electron diffraction (UED). (Top) 2D image (CCD) and the obtained molecular scattering sM(s) and radial distribution f(r) functions: (red) experimental, (blue) theory. (Bottom) The temporal change observed on a bond population elucidates the structure of the reaction intermediate (shown above as two possibilities). Reference 51.

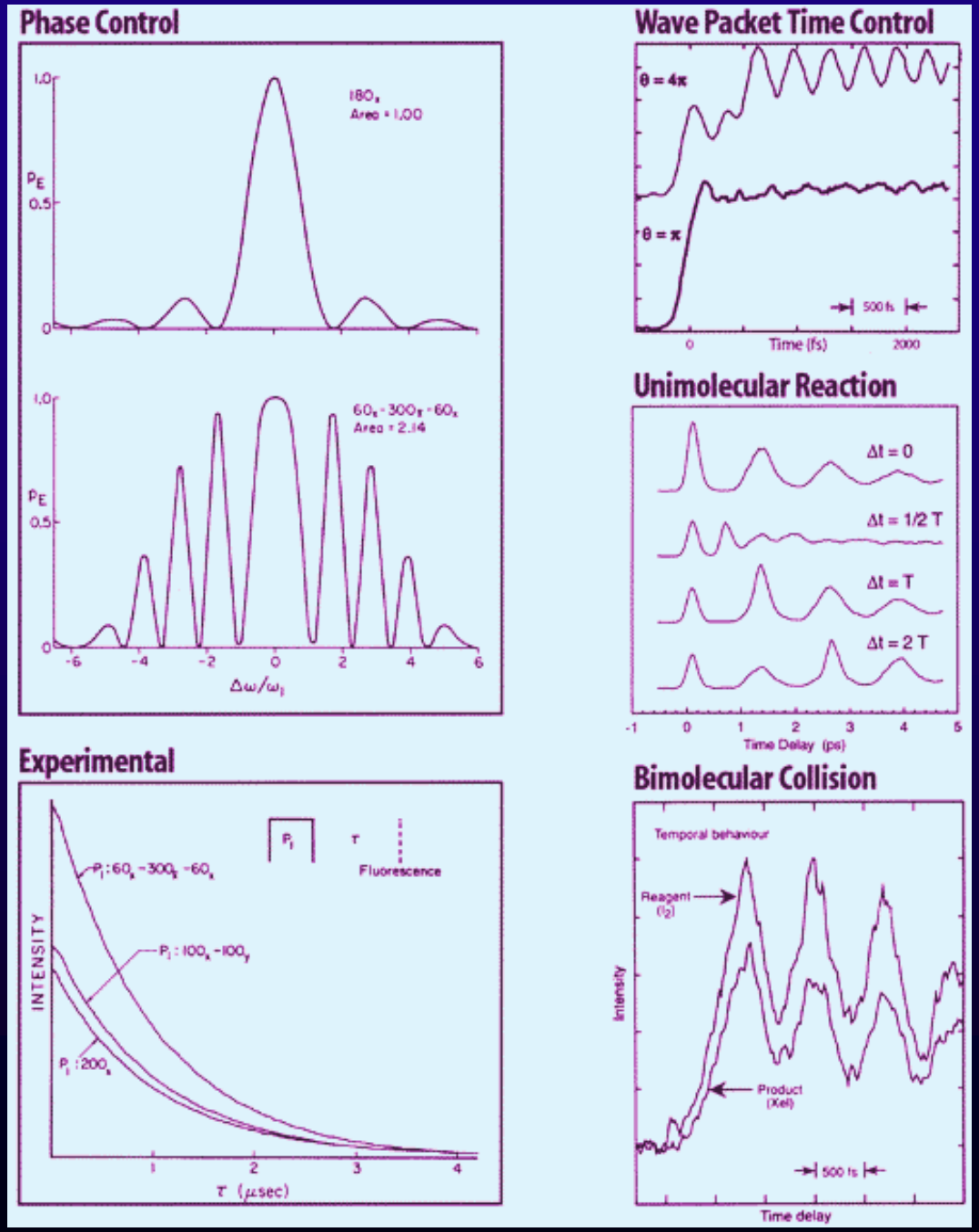

Figure 18

Control by the phase and/or the delay, or the duration of optical pulses. (Left) effect of a designed composite pulse on the fluorescence of a molecule (iodine), showing the large experimental enhancement for the labeled phase-controlled sequence. (Right) control of the population (I2), of unimolecular reactions (NaI), and of a bimolecular collision (Xe + I2); see text. Reference 52.

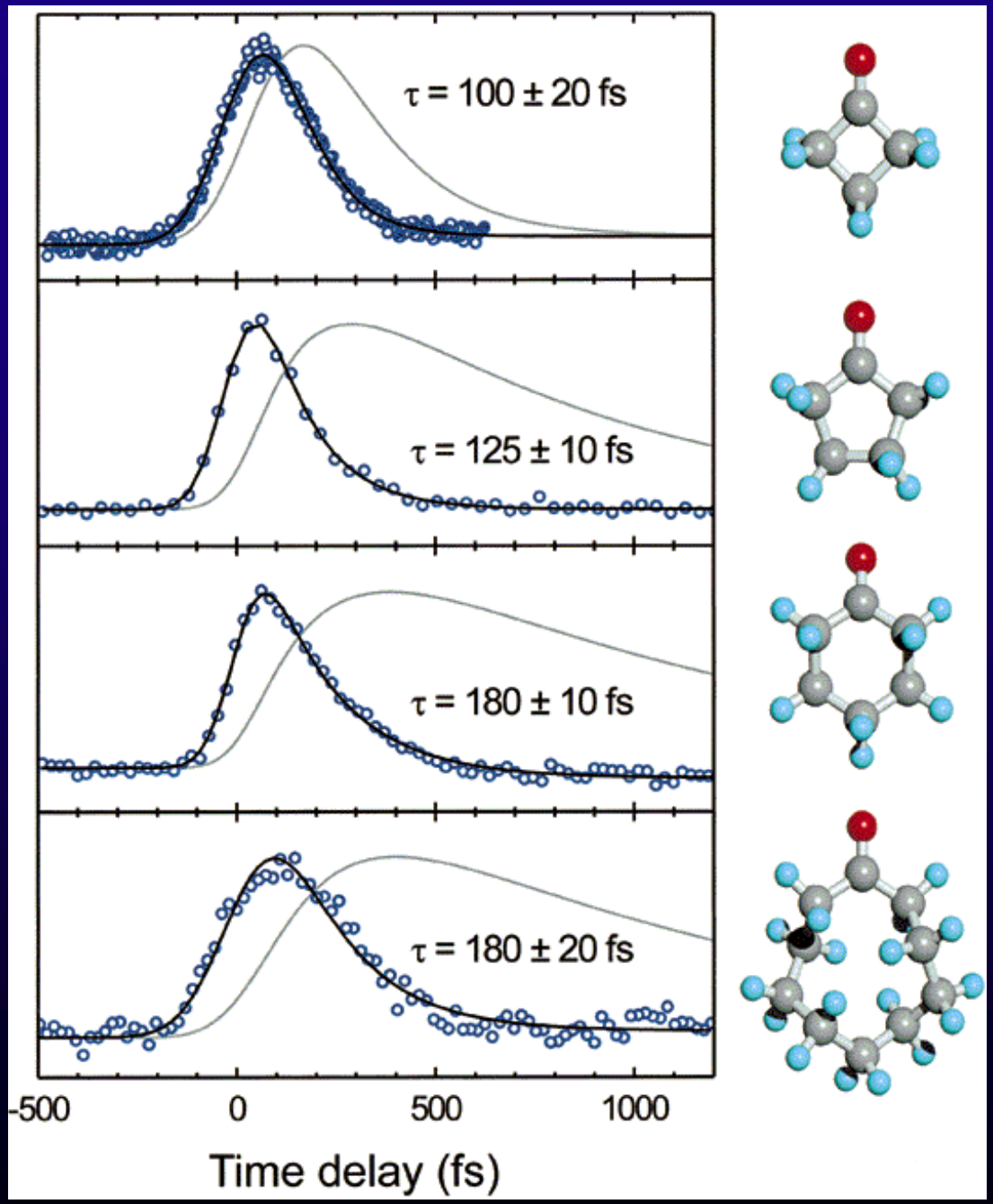

Figure 19

Localized control by femtosecond wave packet preparation at high energies, beating IVR. The series has the same reaction coordinate (C-C bond), but the molecular size has increased in complexity.

Reference 53.

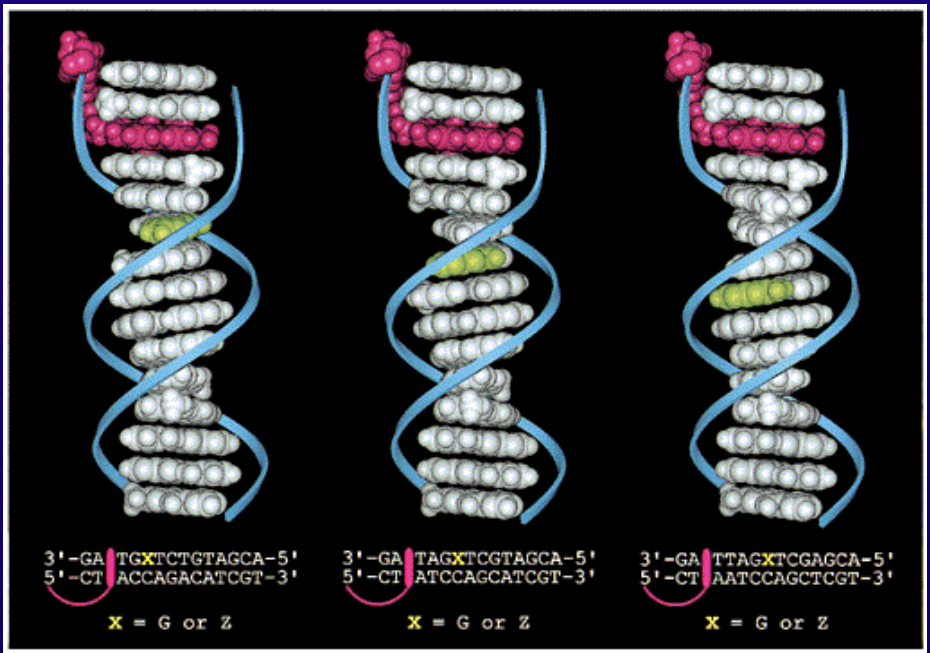

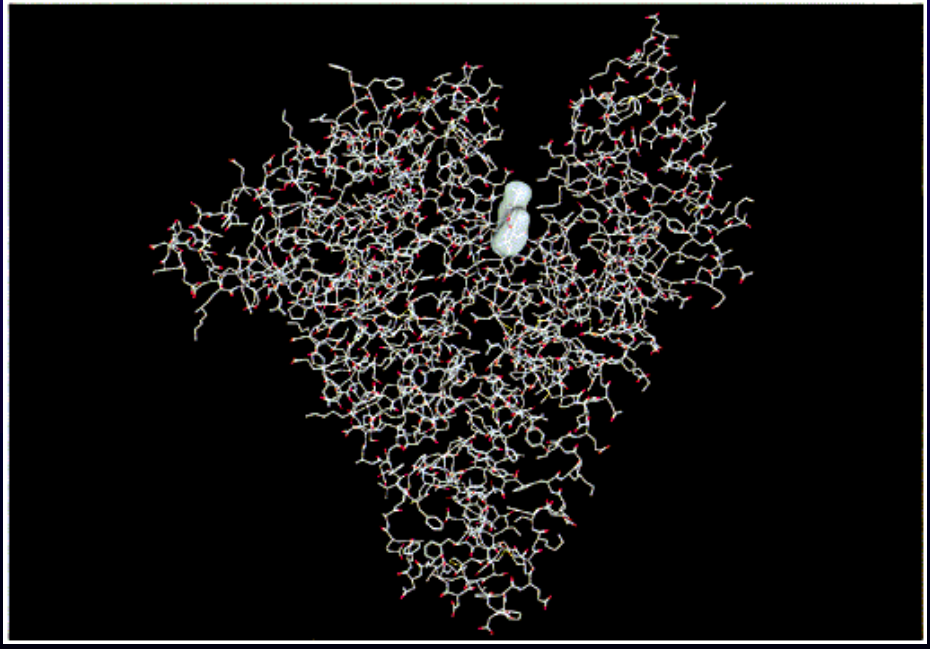

Figure 20

DNA assemblies and protein complexes studied on the femtosecond time scale. Shown are two examples: DNA with donors and acceptors at fixed distances (top) and protein HSA with the molecule HPMO shown in the interior. The focus of research is on electron transfer and molecular dynamics for the former and on probing ligand-recognition effects for the latter. References 54 and 55.

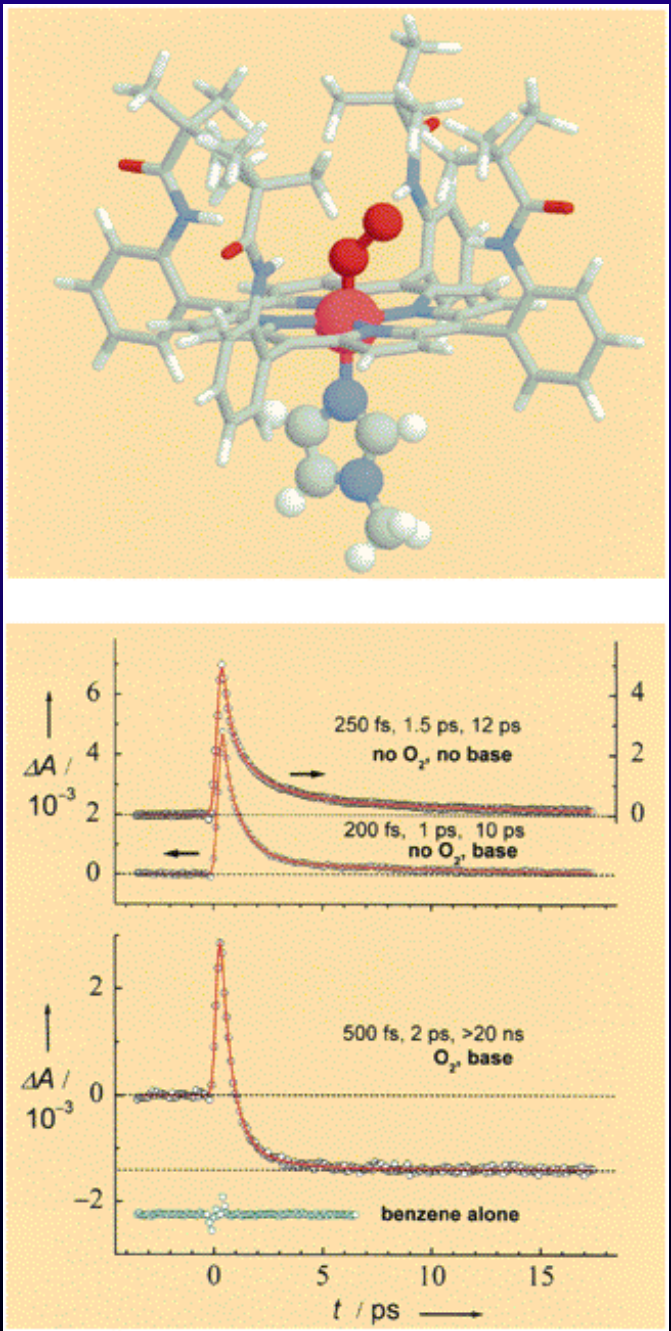

Figure 21

Femtosecond dynamics of model biological systems. Shown here is the structure of dioxygen-picket fence cobalt porphyrin and the femtosecond transients that show the time scales involved and the release of O2 in 1.9 ps at room temperature. The studies on this and the other model systems (not shown) are part of the continued effort in this area. Reference 56.

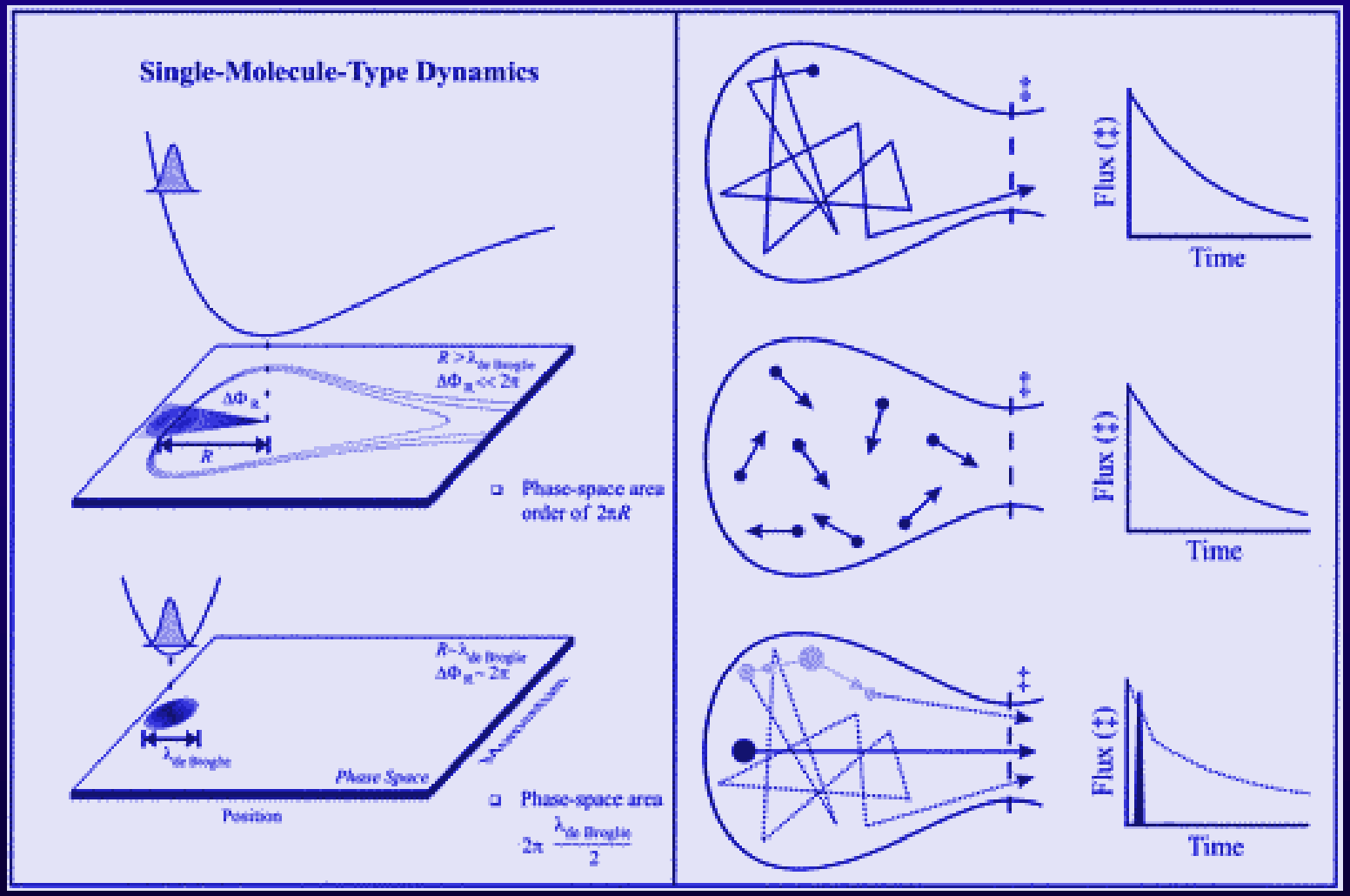

Figure 22 Concept of coherence, both in the dynamics at the atomic scale and in the control of nonstatistical behavior. Shown is the phase space picture, describing the robustness of coherence (left); note the phase-space area of the initial state relative to that of the reaction. (Right) We present, for simplicity, a schematic of a configuration space made of the reactive coordinate and all nonreactive coordinates perpendicular to it (an equivalent phase-space picture can be made). Shown are three cases of interest: (top) the ergodic dynamics, (middle) the incoherent preparation, and (bottom) the coherent wave packet preparation, showing the initial localization, spatially and temporally, and the bifurcation into direct and indirect reaction trajectories. Recent theoretical work (K. Mller, this laboratory) of the corresponding temporal behavior has elucidated the different regimes for the influence of the initial preparation, from a wave packet to a microcanonical limit.

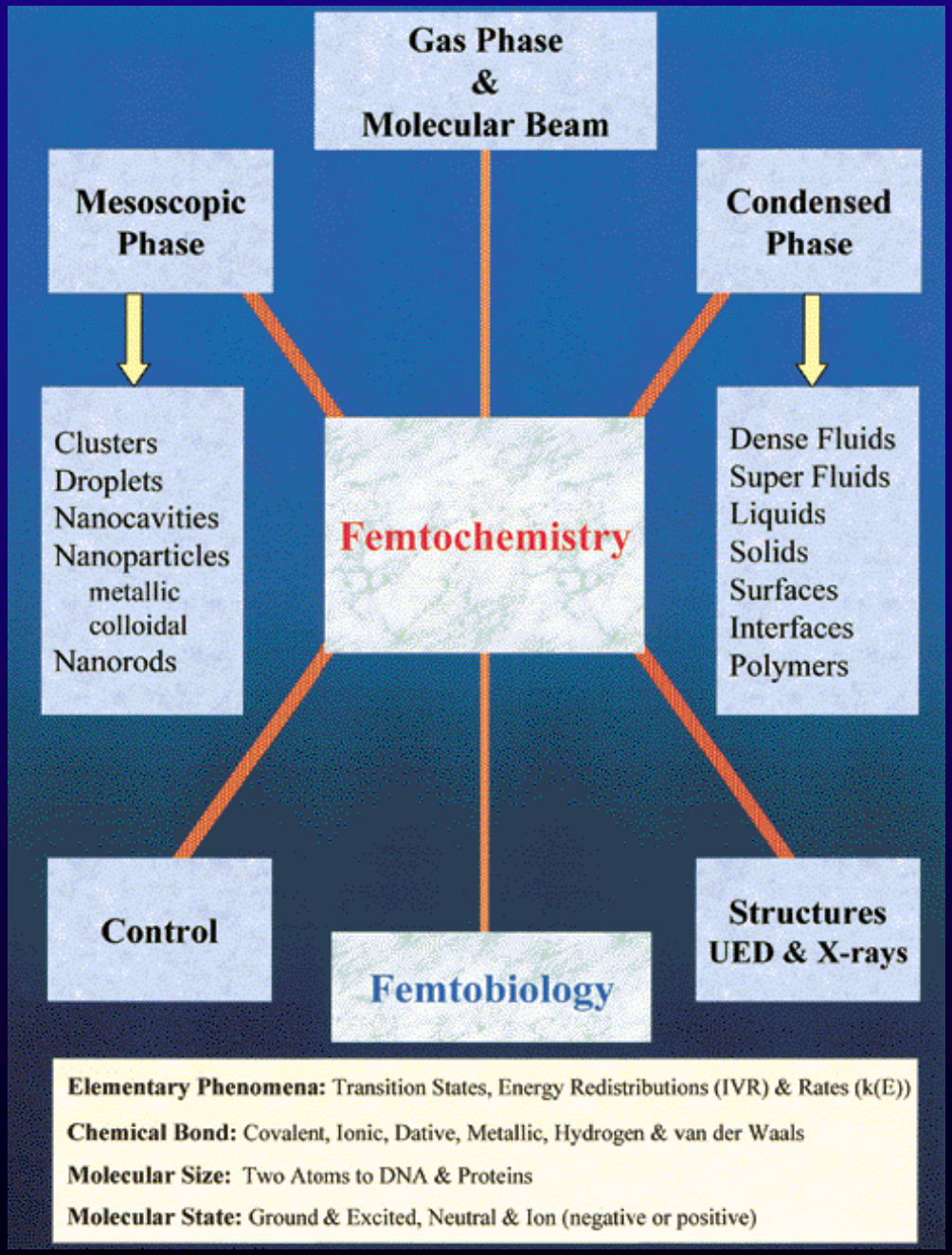

Figure 23

Areas of study in femtochemistry.